Journal of Molecular Catalysis A: Chemical 323 (2010) 23–27

Contents lists available at ScienceDirect

Journal of Molecular Catalysis A: Chemical

journal homepage: www.elsevier.com/locate/molcata

A bonding study of CO–benzene co-adsorption on Rh(1 1 1)

Paula V. Jasen, Estela A. González, Graciela Brizuela, Alfredo Juan*

Departamento de Física, Universidad Nacional del Sur, Av. Alem 1253, Bahía Blanca 8000, Argentina

ARTICLE INFO

Article history:
Received 13 November 2009
Received in revised form 24 February 2010
Accepted 25 February 2010
Available online 15 March 2010

Keywords:
DFT
Benzene
Co-adsorption
Electronic structure

ABSTRACT

The co-adsorption of carbon monoxide and benzene on Rh(1 1 1) has been studied using density functional calculations. We used the ordered p(3 × 30) surface unit cell for the study. Besides, a comparison of the co-adsorption with CO and benzene two-dimensional networks is also given. The hydrogen of the benzene ring presents a bonding angle of 26°. The electronic structure reveals that the CO does not interact with benzene. Regarding the bonding, the Rh–Rh overlap population decreases 36.7% after co-adsorption, which is almost, the same decrease after CO adsorption. The CO–benzene interaction is very weak and a small $H_{benzene}$–C_{CO} OP of 0.001 is detected.

1. Introduction

The adsorption of aromatic molecules on metals is of relevance in several fields of chemical sciences and technology [1,2]. The catalytic conversion of aromatic molecules is an important process in the chemical and petrochemical industries, both for environmental and economical reasons [3,4].

The chemisorption of benzene was studied both experimentally and theoretically at low coverage. On close-packed transition metals bonded benzene lies parallel to the surface through the π electron system [5,6]. The co-adsorption with CO presents ordered structures of benzene on transition metals surfaces and has been experimentally studied on Ru(0 0 0 1) [7,8], Pd(1 1 1) [9,10], Pt(1 1 1) [11,12], Ni(1 0 0) and Ni(1 1 1) [13–16] and Rh(1 1 1) [11,17–19]. In the case of Rh(1 1 1) [11,20], several surface science techniques suggested a 3-fold hollow site for the benzene molecule in presence of CO as an impurity. Theoretical semiempirical methods were used to study the adsorption of benzene on TMS [12,21–23]. On the other hand, ab-initio calculations were performed for benzene on Pt on Ni surfaces [3,24–26].

The co-adsorption of benzene and CO, the subject of this study, provides two additional aspects: mutual structural effects between the different molecules, and contrasting effects on the substrate due to the different adsorbates [27].

Witte et al. studied the low frequency phonon dispersion curves for clear Rh(1 1 1) and ordered monolayers of CO and benzene [28]. HREELS determined that the adsorption is in one configuration instead of a mixture of bridge and hcp structures [11]. STM studies shown that the mobility of benzene decreases in presence of CO observing two ordered domains [29,30]. Rh precovered with CO present a 3 × 3 benzene overlayer with two CO molecules per unit cell [29,30]. LEED experiments examined in detail the co-adsorption either in c(2√3 × 3)Rect or (3 × 3) structures [18,19,31,32]. Morin et al. calculated that the adsorption of benzene with CO-preadsorbed Rh(1 1 1) is more stable on hcp than in bridge location (ΔE = 0.23 eV). This difference is bigger to that obtained in the case of pure benzene adsorption. This can explain the fact that benzene is experimentally found in hcp sites when CO is preadsorbed [33].

Morin et al. have calculated that the adsorption sites for benzene are bridge positions in Pt(1 1 1), while in Pd(1 1 1) and Rh(1 1 1) bridge and hollow position have similar energies values. For the co-adsorption with CO they found the hcp sites as slightly more stable [33].

In this paper, we present a bonding study of the chemisorption of benzene on Rh(1 1 1) based on density functional calculations.

2. Theoretical method

All calculations described herein were performed within the framework of density functional theory (DFT) as implemented in the Amsterdam Density Functional 2000 package (ADF2000) [34]. The molecular orbitals were represented as linear combinations of Slater functions. The gradient correction the Becke [35] approximation for the exchange energy functional and the B3LYP [36] approximation for the correlation functional were employed. In order to increase the computational efficiency, the innermost atomic shells of electrons are kept frozen for every atom except

* Corresponding author. Tel.: +54 291 4595142; fax: +54 291 4595142.
E-mail address: cajuan@uns.edu.ar (A. Juan).

1381-1169/$ – see front matter © 2010 Elsevier B.V. All rights reserved.
doi:10.1016/j.molcata.2010.02.031

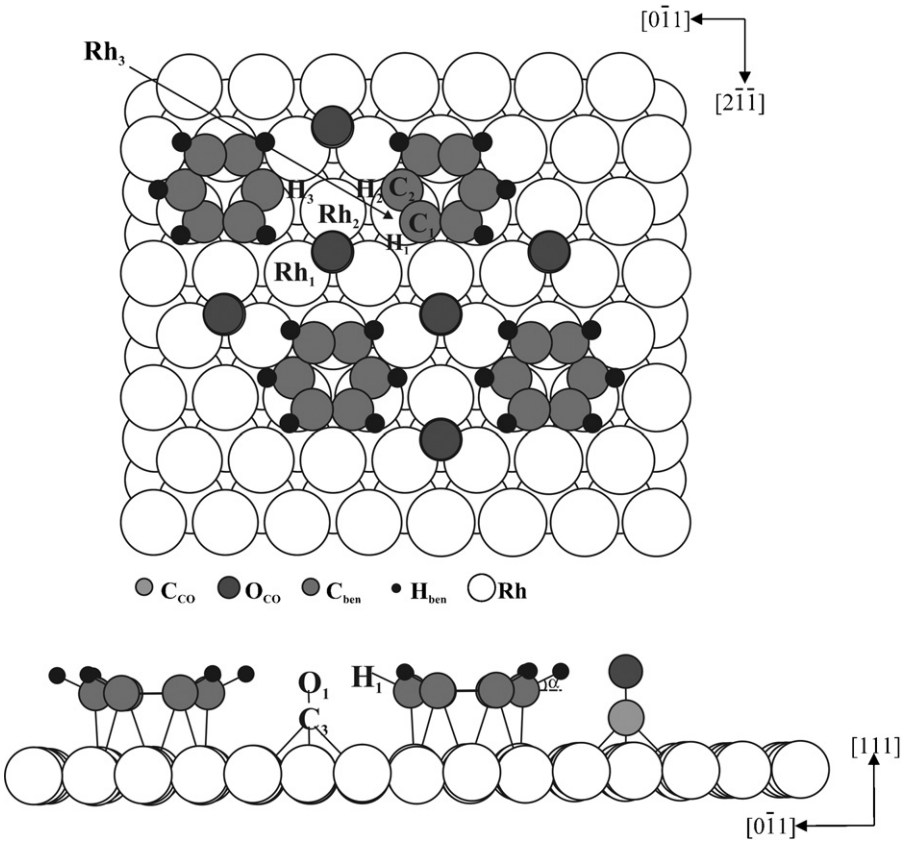

Fig. 1. Schematic top (up) and lateral (down) view of the $(C_6H_6)_4$–$(CO)_6$/Rh system.

hydrogen, since the internal electrons do not contribute significantly to the bonding. We have used a triple-zeta basis set (this means three Slater-type functions for each atomic valence orbital occupied) with polarization functions to express the atomic orbitals of Rh. The basis set of Rh consisted of 4d and 5s orbitals.

Rh is face cubic centered (fcc) metal, and the (1 1 1) surface is the close-packed surface. We used the experimental adsorption geometry determined by Barbieri et al. [27]. The carbon monoxide molecules were taken to stand perpendicular to the surface on hcp sites ring and buckling distortions were also considered. Our computed out-of-plane angle was 26.0°. Morin et al. determined the hcp and bridge adsorption sites have almost the same adsorption energy. Minot et al. showed the hcp is the best configuration on an Rh_6 cluster [23]. Using theoretical calculation Sautet and Joachim proposed the hcp adsorption for benzene [37]. The computed out-of-plane C–H angle was 15° or 32° [33] and 20° [23].

The average perpendicular distance between the aromatic ring and the first Rh layer is 2.070 Å. The shortest Rh–Rh bond distance was 2.689 Å. Carbon–hydrogen bond distances are almost the same to that in the gas phase benzene. The CO distance remains similar (+4.6%) to the vacuum value [38]. The supercell chosen corresponds to a p(3 × 3) superstructure of the adsorbed benzene molecule + 2 CO molecule on Rh_{36} (see Fig. 1) [27]. A slab consisting of four layers of metal atoms for the surface was used with the two upper most layers allowed to relax. The vacuum space was set to an equivalent of five layers of metal. The molecules were adsorbed on one side of the slab. In fact, the literature reports the accuracy of this methodology [39,40]. The adsorption energies were calculated taking the difference between the total adsorbate/surface system and the individual surface and individual adsorbate. The calculated lattice constant in bulk Rh a = 3.845 Å compare well with the experimental values (3.803 Å).

Table 1
Electron density, overlap population (OP), charge and distances for a Rh, a (C_6H_6) and a (CO) clusters.

Structure	Electron orbital occupation			Bond type	OP	Distance (Å)
	s	p	d			
Rh						
Rh_1	0.45	0.29	8.06	Rh_1–Rh_2	0.199	2.689
$(C_6H_6)_4$ ideal lattice[a]						
H_1	0.68	0.00	0.00	C_1–C_2	0.611	1.367
C_1	0.94	1.33	0.00	C_1–H_1	0.580	1.090
$(CO)_6$ ideal lattice[a]						
C_3	0.43	0.36	0.00	C_3–O_1	0.815	1.180
O_1	1.63	3.58	0.00			

[a] The ideal lattice is an hypothetical network considered only benzene or CO in the same arrangement as in the adsorbed state without the metal layers.

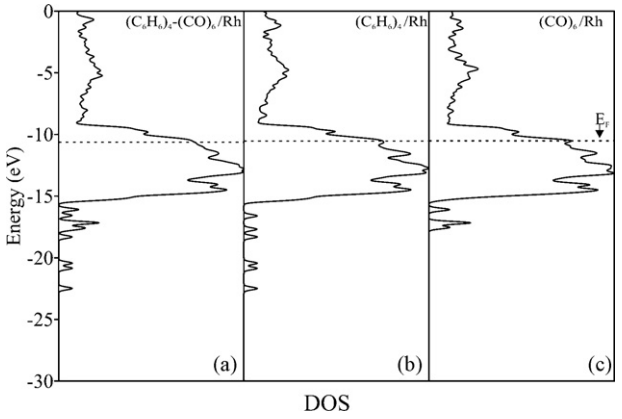

Fig. 2. Total DOS curves for $(C_6H_6)_4$–$(CO)_6$/Rh (a), $(C_6H_6)_4$/Rh (b), and $(CO)_6$/Rh (c).

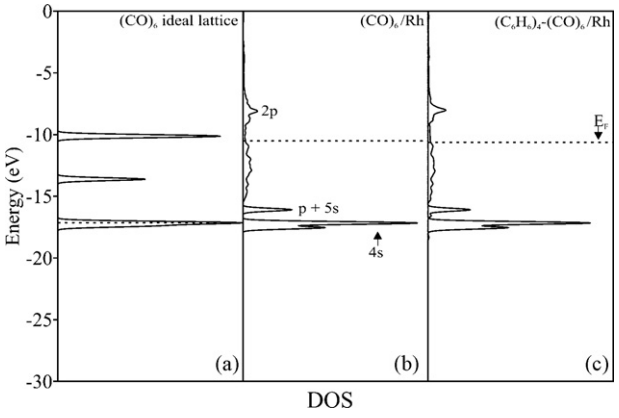

Fig. 3. Total DOS curves for $(CO)_6$ in an ideal lattice (a), a $(CO)_6$/Rh (b), and a $(C_6H_6)_4$–$(CO)_6$/Rh (c) projected DOS on carbon monoxides.

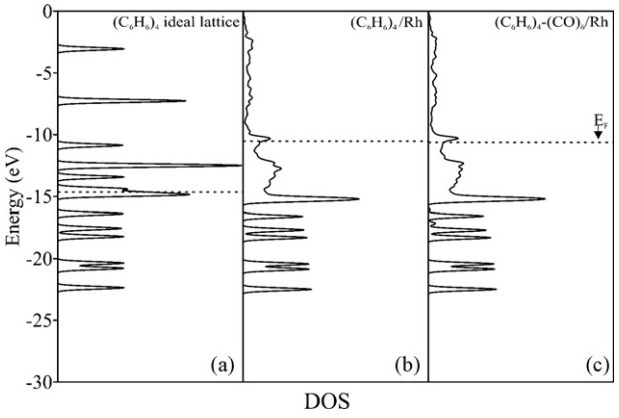

Fig. 4. Total DOS curves for $(C_6H_6)_4$ in an ideal lattice (a), a $(C_6H_6)_4$/Rh (b), and a $(C_6H_6)_5$–$(CO)_6$/Rh (c) projected DOS on benzene.

To understand the Rh–C_6H_6–CO interactions we used the concept of density of states (DOS) and overlap population density of states (OPDOS). The DOS curve is a plot of the number of orbitals as a function of the energy. The integral of the DOS curve over an energy interval gives the number of one-electron states in that interval; the integral up to the Fermi level (E_F) gives the total number of occupied molecular orbitals. If the DOS is weighed with the overlap population between two atoms the overlap population density of states OPDOS is obtained. The integration of the OPDOS curve up to E_F gives the total overlap population of the specified bond orbital and it is a measure of the bond strength. If an orbital at certain energy is strongly bonding between two atoms, the overlap population is strongly positive and OPDOS curve will be large and positive around that energy. Similarly, OPDOS negative around certain energy corresponds to antibonding interactions. The OPDOS curves were computed using the YAeHMOP code [41].

3. Results and discussion

In order to determine the effect of CO and benzene on the Rh(1 1 1) surface structure we first investigated the bare metal surface. We obtained a calculated bulk lattice of a_0 = 3.845 Å. The calculated cohesive energy is −6.15 eV and the Bulk modulus 2.60 Mbar. The experimental values for this are 3.803 Å, −5.80 eV and 2.69 Mbar. These calculated results are in line with previous theoretical calculations [42]. For the clean Rh surface, we computed a contraction of the two outer interlayer spacing of about 2–1%. These values are in good agreement with those determined by LEED [27]. The results for a clean Rh surface are presented in Table 1. The Rh–Rh distance is 2.689 Å, which is very close to 2.72 computed by Morin et al. [33]. The computed Rh electron orbital occupation is $s^{0.45}$ $p^{0.29}$ $d^{8.06}$ with an overlap population (OP) of 0.199. The width of the d band is approximately 7.20 eV. This value is in good agreement with previous calculations [42,43]. The dispersion of the s and p band is much larger than that of the d band, reflecting the more contracted nature of d orbitals. The adsorption energy for benzene in presence of CO is −1.42 eV for the bridge site, which is very close to that computed by Morin et al. [33].

The total DOS of the co-adsorbed system in Fig. 2 presents a series of peaks below −5 eV that belongs to benzene and CO molecules as can be seen by comparison with Fig. 3 (CO) and Fig. 4 (benzene).

To study the CO and benzene contribution to the DOS, we simulated a CO (or benzene) network in vacuum (Figs. 3 and 4a) and an adsorbed CO (benzene) on Rh alone, in the same location as in the co-adsorbed system. It should be mentioned that the E_F for ideal

Table 2
Electron density, overlap population (OP), charge and distances for a $(C_6H_6)_4$/Rh and a $(CO)_6$/Rh clusters.

Structure	Electron orbital occupation			Bond type	OP	Distance (Å)
	s	p	d			
Rh–$(C_6H_6)_4$						
Rh	0.38	0.27	7.42	Rh_3–Rh_2	0.189	2.690
H	0.93	0.00	0.00	C_1–C_2	0.959	1.367
C	0.95	2.87	0.00	C_1–H_1	0.832	1.090
				Rh_3–C_1	0.200	2.199
Rh–$(CO)_6$						
Rh	0.48	0.35	7.56	Rh_1–Rh_2	0.120	2.689
C	1.01	2.51	0.00	C_3–O_1	0.731	1.180
O	1.63	5.75	0.00	Rh_1–C_3	0.529	2.104
				Rh_1–O_1	0.000	3.028

Table 3
Electron density, overlap population (OP), charge and distances for a $(C_6H_6)_5$–$(CO)_7$/Rh cluster.

Structure	Electron orbital occupation			Bond type	OP	Distance (Å)
	s	p	d			
Rh–$(C_6H_6)_4$–$(CO)_6$						
Rh_1	0.46	0.33	7.41	Rh_1–Rh_2	0.126	2.689
Rh_3	0.38	0.27	7.31	Rh_3–Rh_2	0.188	2.690
$H_{benzene}$	0.92	0.00	0.00	C_1–C_2	0.961	1.367
$C_{benzene}$	0.95	2.85	0.00	C_1–H_1	0.827	1.090
				Rh_3–C_3	0.196	2.199
C_{CO}	1.00	2.43	0.00	C_3–O_1	0.740	1.180
O_{CO}	1.63	5.75	0.00	Rh_1–C_3	0.523	2.104
				Rh_1–O_1	0.000	3.028

$(CO)_6$ network present discrete molecular states because no CO–CO interaction is developed and the corresponding E_F is similar to the HOMO state of the CO molecule in vacuum (see Fig. 3a). In the case of the ideal $(C_6H_6)_4$ network, the difference in the E_F is 3.47 eV (see Fig. 4a). The $(C_6H_6)_4$ network behave similar to benzene molecular states due to a very low molecular interaction. When CO or C_6H_6 is considered on the Rh surface, the E_F changes are very small because the weight of the Rh metal states is bigger than the contribution from the adsorbate ($\Delta E_F \cong 0.19$ eV, see Fig. 1). By examining the quantum states in CO/Rh(1 1 1), we found that the first peak in Fig. 3 mainly contains a CO 4σ character with a weak metal d-character. The second peak was found to consist of two types of states: (1) mixing states with strong CO 1π and weak metal d-character; (2) mixing states with strong CO 5σ and quite strong metal d-character. The quantum states dispersed above Fermi level (E_F) mainly contain a strong 2π character of CO and metal d-character. The peak at −10 eV (CO 2π) becomes hybridized with the metal orbitals in the range (−8, −15) eV while the peak at −13.6 eV (CO 1π + 5σ) is shifted to −16.1 eV.

The benzene network interacts with the metal orbitals above −15.6 eV and with CO in a small peak at −17.18 eV. Similar results were reported by Zhang et al. [44]. The almost no-broadening in the CO peaks supports the idea of a low CO–benzene interaction. Table 1 also shows the bond distances. The Rh–$C_{benzene}$ distance of 2.199 Å agrees with the reported bond length of (2.30 ± 0.15) Å [19] and those computed by Morin et al. [33].

Compared to the free CO molecule, the C–O bond on Rh(1 1 1) is elongated from 1.128 to 1.180 Å, which is consistent with the generally accepted explanation that when CO adsorbs on metal surfaces, the C–O bond is weakened. Therefore, our calculated results are in good agreement with experiments.

The C–C distance for the benzene molecule also changes from 1.40 to 1.367 Å (short bond) and 1.506 (long bond) in the adsorbed state in agreement with LEED measurement [27].

Table 2 presents the electron orbital occupation and OP when benzene or CO is adsorbed alone on Rh(1 1 1). The Rh atoms depopulated while benzene and CO atoms increase the electron occupation. The Rh–Rh OP decreases from 0.199 to 0.189, and the C–$C_{benzene}$ increase from 0.611 to 0.959 in both the short and long bonds. As mentioned before the CO bond OP change from 0.815 to 0.731 showing the population of antibonding orbital of CO with an electron transference from Rh. The Rh–Rh OP decreases to 0.120. The Rh–C_{CO} OP is 0.529 at 2.104 Å.

Regarding the bonding, the metal–metal bond OP decreases from 0.199 in the clean Rh surface (see Table 1) to 0.120 when $(CO)_6$ is adsorbed alone on Rh (see Table 2) and 0.126 in the case of Rh–$(C_6H_6)_4$–$(CO)_6$ system (see Table 3). These two mentioned system present a similar reduction in the Rh–Rh OP. In the case of the Rh–(C6H6)4. The Rh–Rh OP remains almost the same as in the clean metal (less than 5%). The OPDOS curves are very similar after adsorption, increasing the antibonding contribution near the E_F. In the case of Rh–C bond interaction with both benzene and CO are almost bonding. For the co-adsorbed system, the Rh–C_{CO} and Rh–$C_{benzene}$ seem similar to that for CO or benzene alone adsorbed over the substrate (see Fig. 5), which can be interpreted as a very low CO–benzene electronic interaction.

For the adsorbed benzene, the C–C bond increases its OP from 0.611 to 0.959 (+56.9%) and finally to 0.961 (+57.3%). The empty

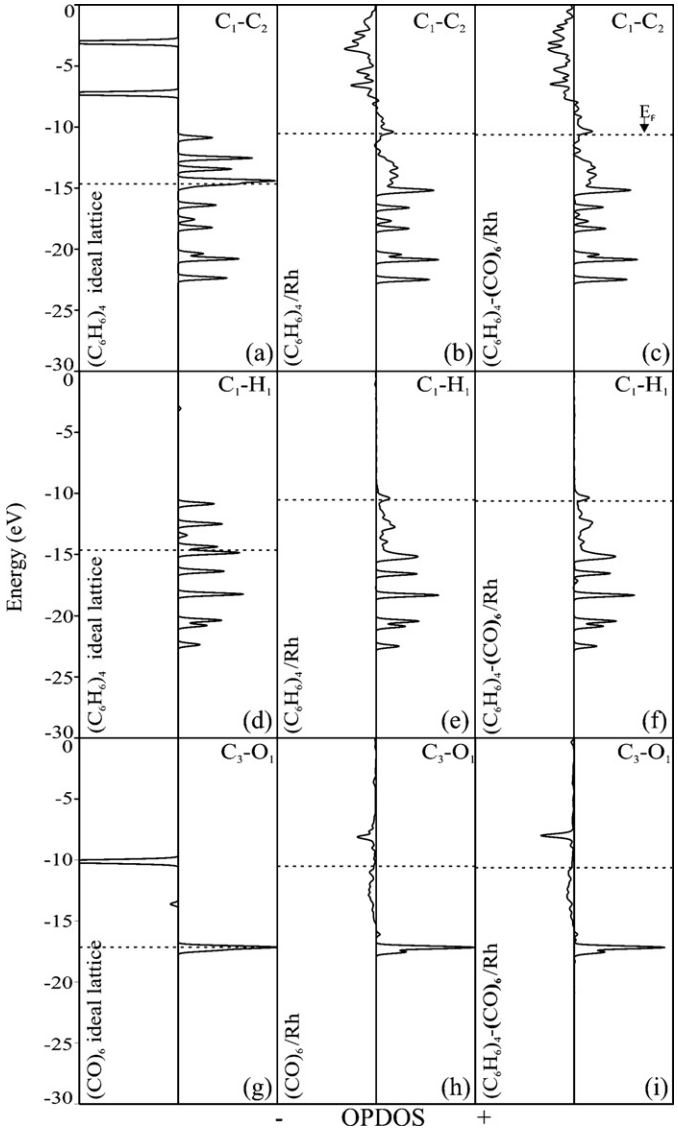

Fig. 5. OPDOS curves for: C_1–C_2 bond in an ideal lattice (a), in $(C_6H_6)_4$/Rh (b) and in $(C_6H_6)_4$–$(CO)_6$/Rh (c); C_1–H_1 bond in an ideal lattice (d), in $(C_6H_6)_4$/Rh (e) and in $(C_6H_6)_4$–$(CO)_6$/Rh (f); C_3–O_1 bond in an ideal lattice (g), in $(CO)_6$/Rh (h) and in $(C_6H_6)_4$–$(CO)_6$/Rh (i).

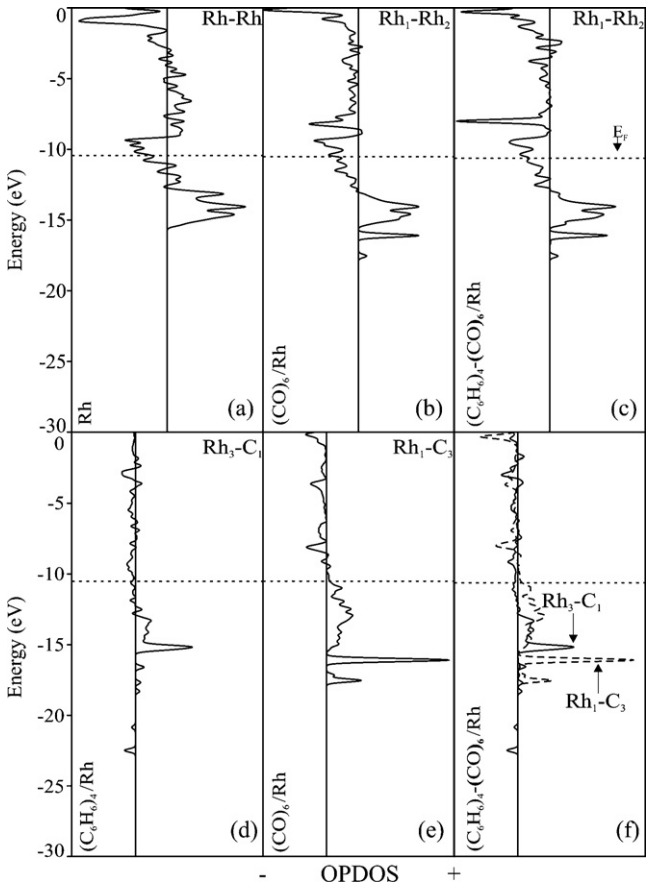

Fig. 6. OPDOS curves for: Rh–Rh bond in pure metal (a), in $(CO)_6$/Rh (b) and in $(C_6H_6)_4$–$(CO)_6$/Rh (c); Rh_3–C_1 bond in $(C_6H_6)_4$/Rh (d); Rh_1–C_3 bond in $(CO)_6$/Rh (e); Rh_3–C_1 (right line) and Rh_1–C_3 (dashed line) bonds in $(C_6H_6)_4$–$(CO)_6$/Rh (f).

orbital for the C–C in vacuum are bonding (up to −10 eV), the shift in the Fermi level due to electron states and then the OP increases. When CO is considered, the situation is similar and some of the small bonding peaks also appear (see Fig. 6). A similar explanation can be given for the increase in the C–H bond OP from 0.580 to 0.832. A small decrease in C–H bond OP (−0.6%) is due to a very small $H_{benzene}$–C_{CO} interaction which is only 0.001. In the case of H–H interaction coming from different benzene molecules changes from 0.002 to 0.001, which do not suffer further changes with CO.

4. Conclusions

We analyzed the CO–benzene co-adsorption on Rh(1 1 1). Starting from experimental information, we have computed a C–H ring angle of 26.0°. The DOS plots shows that the CO–benzene interaction is very weak; however, it is more important than those in the isolated adsorbed system. The metal–metal bond overlap population (OP) decreases 36.7% in the co-adsorbed system. The C–C bond OP within the benzene ring increases with or without CO on Rh. On the other hand, CO changes in its orbitals on the Rh(1 1 1) layer. Our calculations are in agreement with previous experimental data of Barbieri et al. [27] and theoretical calculation of Morin et al. [33].

Acknowledgements

Our work was supported by SGCyT Universidad Nacional del Sur, PICT 1186 and 560 and PIP-CONICET 2009.

References

[1] G.A. Somorjai, Chemistry in Two Dimensions: Surface, Cornell University Press, Itacha, 1981.
[2] C.N. Satterfield, Heterogeneous Catalysis in Industrial Practice, 2nd ed., McGraw-Hill, New York, 1991.
[3] M. Sayes, M.F. Reyniers, G.B. Marin, M. Neurock, J. Phys. Chem. B 106 (2002) 7489.
[4] M. Sayes, M.-F. Reyniers, M. Neurock, G.B. Marin, J. Phys. Chem. B 107 (2003) 3844.
[5] N. Sheppard, Annu. Rev. Phys. Chem. 39 (1988) 589.
[6] F.P. Netzer, Langmuir 7 (1991) 2544.
[7] P. Jakob, D. Menzel, Surf. Sci. 235 (1990) 15.
[8] P.A. Heimann, P. Jakob, T. Pache, H.-P. Steinrück, D. Menzel, Surf. Sci. 210 (1989) 282.
[9] H. Ohtani, M.A. Van Hove, G.A. Somorjai, J. Phys. Chem. 92 (1988) 3974.
[10] H. Ohtani, B.E. Bent, C.M. Mate, M.A. Van Hove, G.A. Somorjai, Appl. Surf. Sci. 33/34 (1988) 254.
[11] C.M. Mate, G.A. Somorjai, Surf. Sci. 160 (1985) 542.
[12] P.V. Jasen, G. Brizuela, Z. Padín, E.A. Gonzalez, A. Juan, Appl. Surf. Sci. 236 (2004) 394.
[13] P.M. Blass, S. Akhter, J.M. White, Surf. Sci. 191 (1987) 406.
[14] H.-P. Steinrueck, W. Huber, T. Pache, D. Menzel, Surf. Sci. 218 (1989) 293.
[15] W. Huber, P. Zebisch, T. Bornemann, H.-P. Steinrueck, Surf. Sci. 258 (1991) 16.
[16] W. Huber, H.-P. Steinrueck, T. Pache, D. Menzel, Surf. Sci. 217 (1989) 103.
[17] E. Bertel, G. Rosina, F.P. Netzer, Surf. Sci. 172 (1986) L515.
[18] M.A. Van Hove, R.F. Lin, G.A. Somorjai, J. Am. Chem. Soc. 108 (1986) 2532.
[19] R.F. Lin, G.S. Blackman, M.A. Van Hove, G.A. Somorjai, Acta Crystallogr. B 43 (1987) 368.
[20] B.E. Koel, J.E. Crowell, C.M. Mate, G.A. Somorjai, Phys. Rev. Lett. 88 (1984) 1988.
[21] A.B. Anderson, M.R. Mc.Devitt, F.L. Urbach, Surf. Sci. 146 (1984) 80.
[22] E.L. Garfunkel, C. Minot, A. Gavezzotti, M. Simonetta, Surf. Sci. 167 (1986) 177.
[23] C. Minot, M.A. Van Hove, G.A. Somorjai, Surf. Rev. Lett. 3 (1995) 285.
[24] C. Morin, M.A. Van Hove, P. Sautet, J. Phys. Chem. B 107 (2003) 2995.
[25] F. Mittendorfer, J. Hafner, Surf. Sci. 472 (2001) 133.
[26] S. Yamagashi, S.J. Jenkins, D.A. King, J. Chem. Phys. 114 (2001) 5765.
[27] A. Barbieri, M.A. Van Hove, G.A. Somorjai, Surf. Sci. 306 (1994) 261.
[28] G. Witte, H. Range, J.P. Toennies, Ch. Wöll, J. Electron Spectrosc. Relat. Phenom. 64–65 (1993) 715–723.
[29] H.A. Yoon, M. Salmeron, G.A. Somorjai, Surf. Sci. 373 (1997) 300.
[30] H. Ohtani, R.J. Wilson, S. Chiang, C.M. Mate, Phys. Rev. Lett. 60 (1988) 2398.
[31] R.F. Lin, R.J. Koestner, M.A. Van Hove, G.A. Somorjai, Surf. Sci. 134 (1983) 161.
[32] M.A. Van Hove, R.F. Lin, G.A. Somorjai, Phys. Rev. Lett. 51 (1983) 778.
[33] C. Morin, D. Simon, P. Sautet, J. Phys. Chem. B 108 (2004) 5653.
[34] Amsterdam Density Functional Package Release, Vrije Universiteit, Amsterdam, 2001.
[35] D. Becke, Phys. Rev. A 38 (1988) 3098–3100.
[36] C. Lee, W. Yang, R.G. Parr, Phys. Rev. B 37 (1988) 785–789.
[37] P. Sautet, C. Joachim, Chem. Phys. Lett. 185 (1991) 23.
[38] O.R. Gillian, C.M. Johnson, W. Gordy, Phys. Rev. 78 (1950) 140.
[39] B. Hammer, J.K. Nørskov, Adv. Catal. 45 (2000) 71.
[40] Q. Ge, R. Kose, D.A. King, Adv. Catal. 45 (2000) 207.
[41] G. Landrum, W. Glassey, Yet Another Extended Hückel Molecular Orbital Package (YAeHMOP), Cornell University, 2001, YAeHMOP is freely available on the World Wide Web at http://overlap.chem.cornell.edu:8080/yahemop.html.
[42] M.V. Ganduglia-Pirovano, M. Scheffler, Phys. Rev. B 59 (1999) 15533.
[43] E. Hüger, K. Osuch, Solid. State Commun. 131 (2004) 175.
[44] C.J. Zhang, P. Hu, M.-H. Lee, Surf. Sci. 432 (1999) 305.